



USING HIGH RESOLUTION SATELLITE IMAGERY TO DETECT DAMAGE FROM THE 2003 NORTHERN ALGERIA EARTHQUAKE

Ellen RATHJE¹ and Melba CRAWFORD²

SUMMARY

The Northern Algeria ($M_w = 6.8$) earthquake occurred on 21 May 2003 and affected a large coastal region in Algeria. This event is one of the first large earthquakes to be imaged immediately thereafter by a high-resolution commercial satellite, and therefore, represents a unique opportunity to evaluate whether detailed earthquake damage can be accurately identified from high-resolution satellite images. High-resolution (0.6 m), pre- and post-earthquake images of the severely damaged Algerian city of Boumerdes were acquired by the Quickbird satellite and used for this study. Semi-automated, thematic classification algorithms were investigated as methods to identify specific collapsed and pancaked buildings using only a post-earthquake, pan-sharpened image. Classifications were performed first using only spectral (color) information, but were then extended to include both spectral and textural information. Supervised classification using spectral and textural signatures provided the most accurate identification of heavily damaged areas in the image. Additionally, change detection algorithms, which compare pre- and post-earthquake images, were investigated. Change detection allowed for a more complete documentation of damage across parts of the city, but also suffered from limitations related to image changes that were not related to the earthquake. A damage map of Boumerdes developed from the satellite images revealed that the heaviest damage was concentrated in the southwestern part of the city. The results of this study indicate that high-resolution satellite images analyzed using semi-automated classification algorithms, or simple visual classification, are potentially useful for identifying areas exhibiting severe earthquake damage.

INTRODUCTION

With the recent successful launch of high-resolution commercial satellites, the ability to identify earthquake-induced damage from satellite imagery is a reality. Digital data from high-resolution commercial satellites have spatial resolutions as high as 0.6 m, and therefore, these data potentially contain a wealth of information for mapping earthquake damage. Several methodologies developed in image and signal processing for thematic mapping and monitoring change in multi-temporal data sets can be utilized to extract this information. Two widely used approaches are: (1) thematic classification and (2) change detection. Both approaches have advantages and disadvantages with respect to their ability to

¹ Assistant Professor, University of Texas, Austin, TX, USA. Email: e.rathje@mail.utexas.edu

² Engineering Foundation Endowed Professor #1, University of Texas, Austin, TX, USA. Email: crawford@csr.utexas.edu

provide the necessary information for earthquake reconnaissance and earthquake response over a large areal extent.

This study used pre- and post-earthquake satellite images from the 21 May 2003 Northern Algeria ($M_w = 6.8$) earthquake as a test bed for demonstrating the ability to identify earthquake damage from satellite images. Pre- and post-event images of the city of Boumerdes, a small coastal city severely affected by the earthquake, were obtained from the Quickbird satellite (www.digitalglobe.com). Both semi-automated thematic classification methods and change detection methods based on visual examination were investigated to identify damage in the images.

DAMAGE DETECTION METHODOLOGIES

Over the last few years the remote sensing field has advanced significantly with the launch of high-resolution commercial satellites, such as Quickbird in 2001 (www.digitalglobe.com) and IKONOS in 1999 (www.spaceimaging.com). These satellites carry sensors that collect digital image data at spatial resolutions of 0.6 m (Quickbird) to 1 m (IKONOS), which allows identification of terrestrial features such as individual buildings, roads, and even cars. These satellites acquire panchromatic data (a single band between 450-900 nm in the electromagnetic spectrum, usually displayed as gray-scale) at high resolution (0.6 to 1.0 m), as well as multispectral data at lower resolution (2.8 to 4.0 m). The multispectral sensors on these platforms collect data in distinct spectral bands (blue 450-520 nm, green 520-600 nm, red 630-690 nm, near infrared 760-900 nm) that provide important spectral (color) information about the target. Although the multispectral data are collected at a lower resolution (2.8 m for Quickbird, 4 m for IKONOS), they can be fused with the higher resolution panchromatic data to produce spatially enhanced color images, called pan-sharpened images.

In image analysis, thematic classification involves labeling objects or regions of interest within a digital image using information derived from “features” extracted from the image data [Schowengerdt 1]. Classification of individual pixels (referred to as pixel-by-pixel classification) is based on the values of the features associated with that pixel and is commonly used in remote sensing data analysis. A wide range of methods, including statistical, artificial intelligence, and user-defined rule based methods, have been developed to accomplish the classification task. Thematic classification typically is performed on single images, although sequences of data can be analyzed jointly if available. Earthquake damage detection using solely post-earthquake satellite images essentially involves classifying parts of an image as “damaged” and “undamaged” based on characteristics of the image and uses common classification algorithms. This is an attractive approach for earthquake damage detection because it requires only a post-earthquake image. However, the choice of the characteristics that distinguish between the various regions of interest (often called classes) is extremely critical to the success of the classification. Common characteristics used in thematic classification are spectral responses (e.g., amplitude responses in the blue, green, red, and infrared bands) and texture. Texture is a feature that shows promise in distinguishing between damaged and undamaged areas [Zhang and Xie 2] because it provides information about the “spatial distribution of tonal variations” in an image [Haralick et al. 3]. Further, texture is also a stable characteristic that does not change significantly with illumination, season, or location, unlike spectral (color) characteristics that often vary seasonally with sun angle and vegetation cycles.

Most quantitative textural characteristics are based on statistical measures of the change in tone (or gray scale) across an image area. Second-order statistics derived from the gray-tone co-occurrence matrix (CM) of an image often provide useful information regarding texture [Julesz 4]. The contents of $CM(i,j)$ are the probabilities that a pair of gray levels (i,j) occur at a separation of h units. The separation, h , is defined in terms of a number of pixels and a direction (e.g., horizontal, vertical, diagonal). The probabilities within the CM are referenced as $p(i,j)$. If an image has a “smooth” texture and h is small

compared to the size of the textural elements, pairs of points tend to have similar gray levels. These large numbers of similar gray levels result in large values close to the diagonal of the CM and small values away from the diagonal. If an image has a “rough” texture, then pairs of points tend to have dissimilar gray levels, which results in more scatter about the diagonal within the CM. In the pioneering work of Haralick et al. (1973), a variety of scalar textural measures based on the CM were proposed to quantify the scatter within the CM (e.g., contrast $CON = \sum (i - j)^2 \cdot p(i,j)$, dissimilarity $DIS = \sum |i - j| \cdot p(i,j)$, angular second moment $ASM = \sum p(i,j)^2$, and entropy $ENT = -\sum p(i,j) \cdot \log p(i,j)$). Each extracts different spatial information and is affected differently by the scatter in the CM. CON and DIS are measures of local variation, while ASM is a measure of homogeneity. ENT is a measure of randomness in an image. Haralick et al. [3] and Weszka et al. [5] used these textural measures, as well as combinations of these measures, to classify terrain type from aerial photographs, land use from satellite imagery, and sandstone types from photomicrographs. These texture measures are still used in classification applications today [Schowengerdt 1]. More recently, methods such as Gabor filters [Lamei et al. 6], wavelets [Fukuda and Hirose 7], Markov random fields [Derin and Elliott 8, Manjunath and Chellappa 9, Won and Derin 10], and multi-resolution methods [Bouman and Liu 11, Krishnamachari and Chellappa 12] have become popular for representing texture.

Change detection is another attractive approach for earthquake damage detection because it involves identification of major changes between pre- and post-earthquake images. Singh [13] reviewed traditional semi-automated change detection methods used with digital images. Some frequently used change detection methods include image differencing, image-to-image correlation, image ratioing, and principal component and minimum noise fraction (MNF) analysis. These methods have been used to identify buildings, monitor land use changes, and assess deforestation. Huyck et al. [14] used moderate resolution (20 m by 20 m pixels) pre- and post-earthquake optical satellite images from the 1999 Kocaeli, Turkey earthquake to investigate the ability of change detection to identify earthquake damage. Using post-earthquake reconnaissance damage data, Huyck et al. (2002) characterized the damage distribution across the city of Golcuk. The city was divided into five regions based on the percentage of the building stock that had collapsed during the earthquake. The regions ranged from areas with less than 6% of the building stock collapsed to areas with more than 50% of the building stock collapsed. Image differencing was performed for each of the five defined regions. The results showed that areas with more damage became brighter in the images after the earthquake due to the higher reflectance of rubble. The most significant difference occurred for areas with more than 50% of the buildings collapsed.

Change detection requires that the pre- and post-earthquake images be aligned geometrically (co-registered) and that the impact of differences in sun angle and atmospheric conditions at the times the two images were collected be mitigated. Additionally, the images typically contain changes that are not earthquake related, and thus may incorrectly identify some damaged areas. This issue becomes even more problematic when analyzing high-resolution images because these images contain small-scale features, such as traffic congestion, that are highly transient. Finally, pre-earthquake images may not always be available, and in this case, change detection is not impossible.

Although single-image thematic classification of post-earthquake images does not suffer from the issues noted for change detection algorithms, thematic classification does require the existence of significant distinguishable differences in damaged and non-damaged areas. Thus, only severely damaged and fully collapsed/pancaked buildings typically can be identified via thematic classification.

NORTHERN ALGERIA EARTHQUAKE

Earthquake Effects

The Northern Algeria earthquake ($M_w = 6.8$) occurred on 21 May 2003 along the northern coast of Algeria, east of the capital city of Algiers (Figure 1). The northern coast of Algeria is an area of high seismicity that coincides with the boundary between the Eurasian and African plates. This thrust event occurred on a previously unknown northeast-trending reverse fault that dips predominantly to the south. Preliminary fault rupture inversions indicate that the fault ruptured bilaterally from its epicenter, approximately 30 km to the west and 20 km to the east. The zones of largest slip occurred near the epicenter and near the western terminus of the rupture [EERI 15].

The city of Boumerdes is located approximately 30 km west of the earthquake epicenter, very close to the western terminus of the rupture and a zone of high slip indicated by fault rupture inversions. No ground motions were recorded in Boumerdes during the main shock. However, ground motions recorded 12 to 20 km inland from Boumerdes measured peak ground accelerations in the range of 0.3 to 0.5 g. These motions are consistent with those predicted by current attenuation relationships for reverse events [EERI 15].

The city of Boumerdes was founded in 1958 as an educational and administrative outpost for the capital, Algiers. Because of the relatively recent establishment of the city and the original purpose of establishing the city, the building stock consists mostly of reinforced concrete frame structures constructed by government-owned construction companies [EERI 15]. Approximately 18% of the building stock in Boumerdes was destroyed by the earthquake, with the damage predominantly occurring to large multi-story structures [EERI 15].



Figure 1. Epicenter of the Northern Algeria earthquake and city of Boumerdes [16]

Satellite Data

Three sets of satellite images were obtained from the Quickbird satellite, operated by DigitalGlobe (www.digitalglobe.com). The pre-earthquake image was acquired on 22 April 2002 at an off-nadir angle of 11°. The off nadir angle represents the angle (measured from vertical) at which the sensor was pointed when acquiring an image. As images are acquired at larger off nadir angles, more geometric distortion is observed in an image. Two post-earthquake images were obtained: one acquired on 23 May 2003 (24° off nadir) and the other on 18 June 2003 (8° off nadir). The 23 May 2003 image represents the earliest

possible attempt to capture an image of Boumerdes, but it had a large off nadir angle because of the location of the satellite at that time. By 18 June 2003, the satellite orbit allowed an image of Boumerdes to be collected at a much smaller off-nadir angle. For each date, a 2.8-m resolution multispectral image and a 0.6-m resolution panchromatic image were obtained and fused to create pan-sharpened color images at 0.6-m resolution. Figure 2 is the 23 May 2003 pan-sharpened satellite image of the entire city of Boumerdes.



Figure 2. Pan-sharpened satellite image of Boumerdes acquired on 23 May 2003 (from DigitalGlobe)

IDENTIFICATION OF EARTHQUAKE DAMAGE

Semi-Automated Thematic Classification

Initial investigations focused on using semi-automated thematic classification to identify heavily damaged buildings in a small section of southwestern Boumerdes using only the post-earthquake image. Figure 3 shows the pan-sharpened 23 May 2003 image of this section of Boumerdes. This section of Boumerdes was chosen because fully collapsed structures are readily visible, but many undamaged are also present. Classification of this Boumerdes image focused on trying to accurately identify the five fully collapsed and pancaked structures labeled (a) through (e) in Figure 3. All image analysis was performed with the software ENVI 3.4 [Research Systems, Inc. 17].

Visual inspection of this image indicates that the damaged areas have distinct color (i.e. spectral) characteristics, as well as textural characteristics. The challenge is to identify which characteristics best distinguish between damaged and undamaged areas. For this initial evaluation of distinguishing characteristics, five general classes within the image were defined: (1) collapsed structures and debris, (2) asphalt and undamaged buildings, (3) soil, (4) vegetation, and (5) shadow. Training areas for each class were identified within the image, each area encompassing between 1,000 and 2,000 m². These training areas represent only a small percentage of each class within the image. After defining the training areas, classification was performed with a maximum-likelihood, supervised classification algorithm. In supervised classification, the training data are used to estimate the characteristics/attributes of each class and then the remaining pixels in the image are labeled as one of the defined classes based on the class the

pixel most resembles [Lillesand et al. 18]. A maximum-likelihood classifier assigns the pixel to the class for which the statistical likelihood function is maximized.

The initial supervised classification used only data from the spectral bands (blue, green, red, and near infrared) as input into the classification algorithm. Separability analysis was performed to evaluate the statistical separability of the training classes. The Jeffries-Matusita separability measure [1], which ranges between 0.0 (low separability) and 2.0 (high separability), is reported for each pair of classes. Typically, separability greater than 1.9 is desired. Using only spectral data, the separability analysis indicated low separability (Jeffries-Matusita separability measure between 0.9 and 1.3) for class pairs 1-2 (collapse-asphalt/buildings), 2-3 (asphalt/buildings-soil), and 1-3 (collapse-soil). All other class pairs displayed separability greater than 1.9.

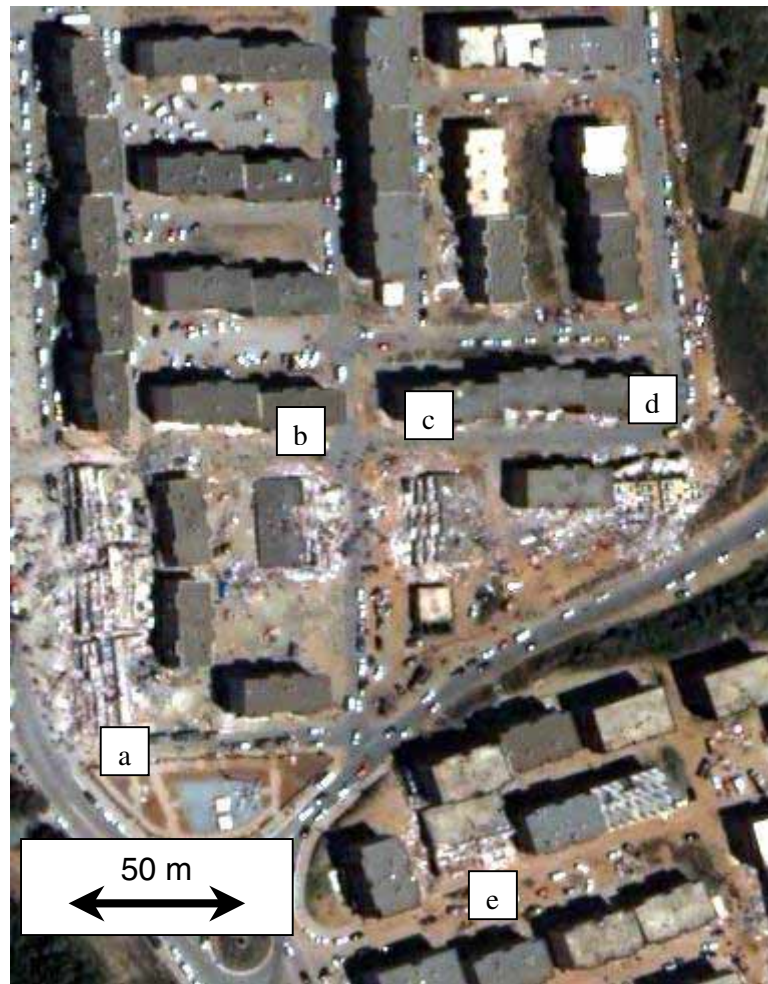


Figure 3. Post-earthquake, pan-sharpened image of southwestern Bouterdes

The resulting maximum-likelihood classification using only spectral data is shown in Figure 4. In this figure the red areas represent collapse and debris (Class 1), the green areas represent undamaged buildings and asphalt (Class 2), the blue areas represent soil (Class 3), the yellow areas represent vegetation (Class 4), and the cyan-blue areas are building shadows (Class 5). Approximately 73% of the collapse area (Class 1), as defined by the five collapsed buildings, is accurately identified as collapse and debris. This corresponds to a 27% omission error. Additionally, approximately 53% of the classified collapse areas

(i.e., red areas in Figure 4) do not correspond to the identified collapse areas. This represents a 47% commission error. These misclassified areas are located predominantly north of the collapsed buildings. Visual examination of Figures 3 and 4 reveals that these areas correspond to regions that have a spectral signature similar to the collapsed areas. Note the white cars and building roofs misclassified as collapse near the top of the image because their color is similar to the collapsed structures. The large commission error for the collapse class (Class 1) is not surprising based on the results of the separability analysis, which indicated that Classes 1 and 2, and Classes 1 and 3 displayed low separability. To better distinguish between damaged and undamaged areas, textural measures were considered in the classification.

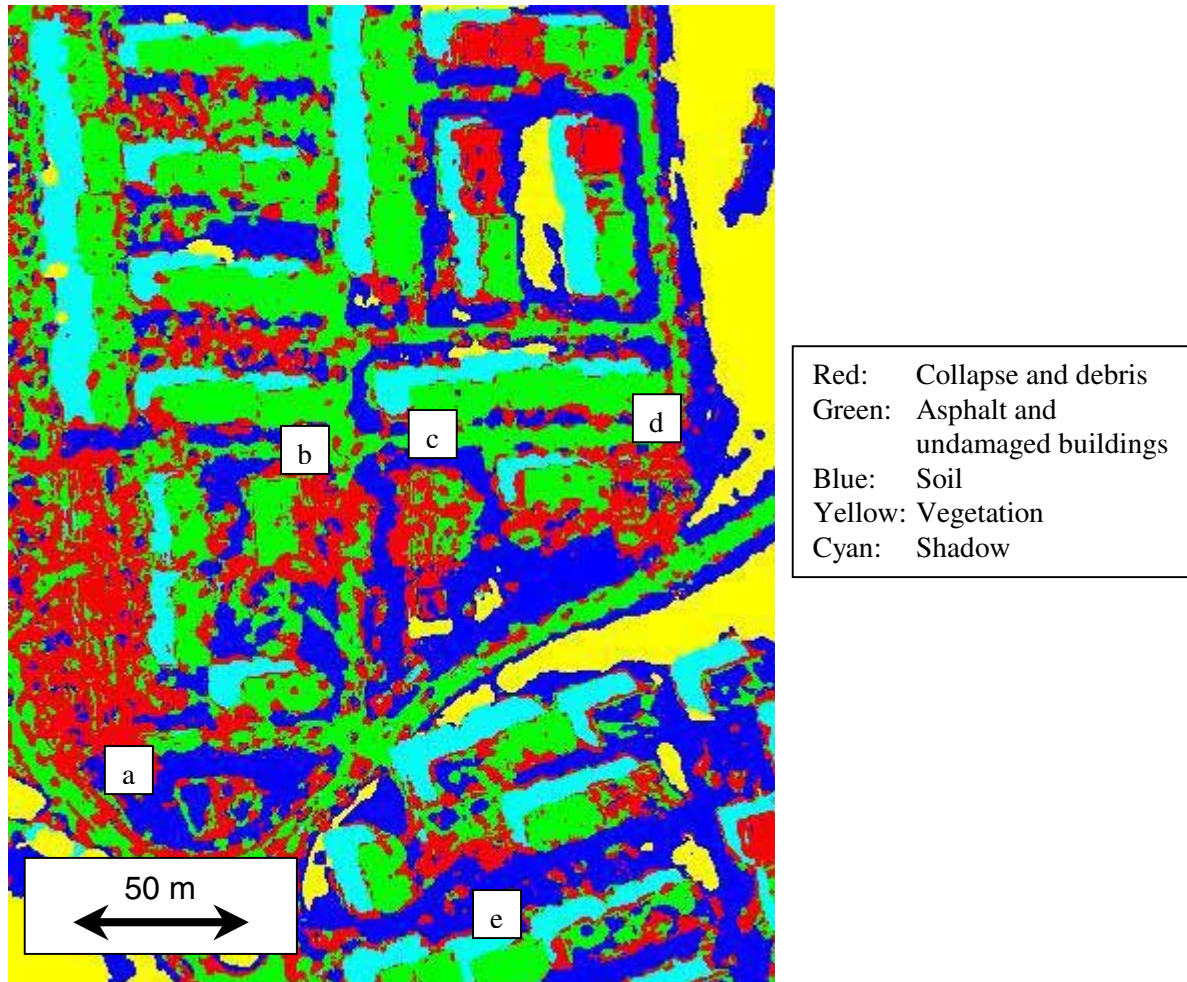


Figure 4. Classification results using only four spectral bands

Texture characteristics are useful in image classification because they are related to the “smoothness” or “roughness” of gray scales across an image. Visual inspection of Figure 3 suggests that collapsed areas have rough texture, with large variations in tone over small distances, while the undamaged areas have smooth texture, with little variation in tone over distance. Therefore, texture should help distinguish collapsed areas from undamaged areas.

As discussed earlier, second-order statistics derived from the gray-tone co-occurrence matrix (CM) provide useful information regarding texture [4]. The elements within the CM are referenced as $p(i,j)$,

where i and j are gray levels. Eight scalar texture measures were computed across the image for a 20 by 20 pixel window, shifted 10 pixels horizontally. Comparing the average texture measures for the five training classes indicated that the collapse areas (Class 1) displayed distinctively large values of contrast, $CON = \sum (i-j)^2 \cdot p(i,j)$, and dissimilarity, $DIS = \sum |i-j| \cdot p(i,j)$. Both CON and DIS quantify the regular scatter about the diagonal in the CM matrix, $p(i,j)$, using weights that increase as $(i-j)$ increases. Separability analysis then was performed using the four spectral bands and the texture measures CON and DIS. The separability for class pairs 1-2 (collapse-asphalt/buildings), 2-3 (asphalt/buildings-soil), and 1-3 (collapse-soil) improved significantly (Jeffries-Matusita separability measures greater than 1.65).

Maximum-likelihood supervised classification was performed using the four spectral bands and the two texture measures CON and DIS. The same training classes from the previous analysis were used. The four spectral bands and the two texture measures were used as input for the classification. The resulting classification using both spectral and textural measures is shown in Figure 5. The collapsed areas are better classified in this analysis, with only a 15% omission error. The commission error (classifying undamaged areas as collapsed areas) is still relatively high, with about 35% of the red areas in Figure 5 representing undamaged areas. However, these areas tend to be spatially distributed throughout the

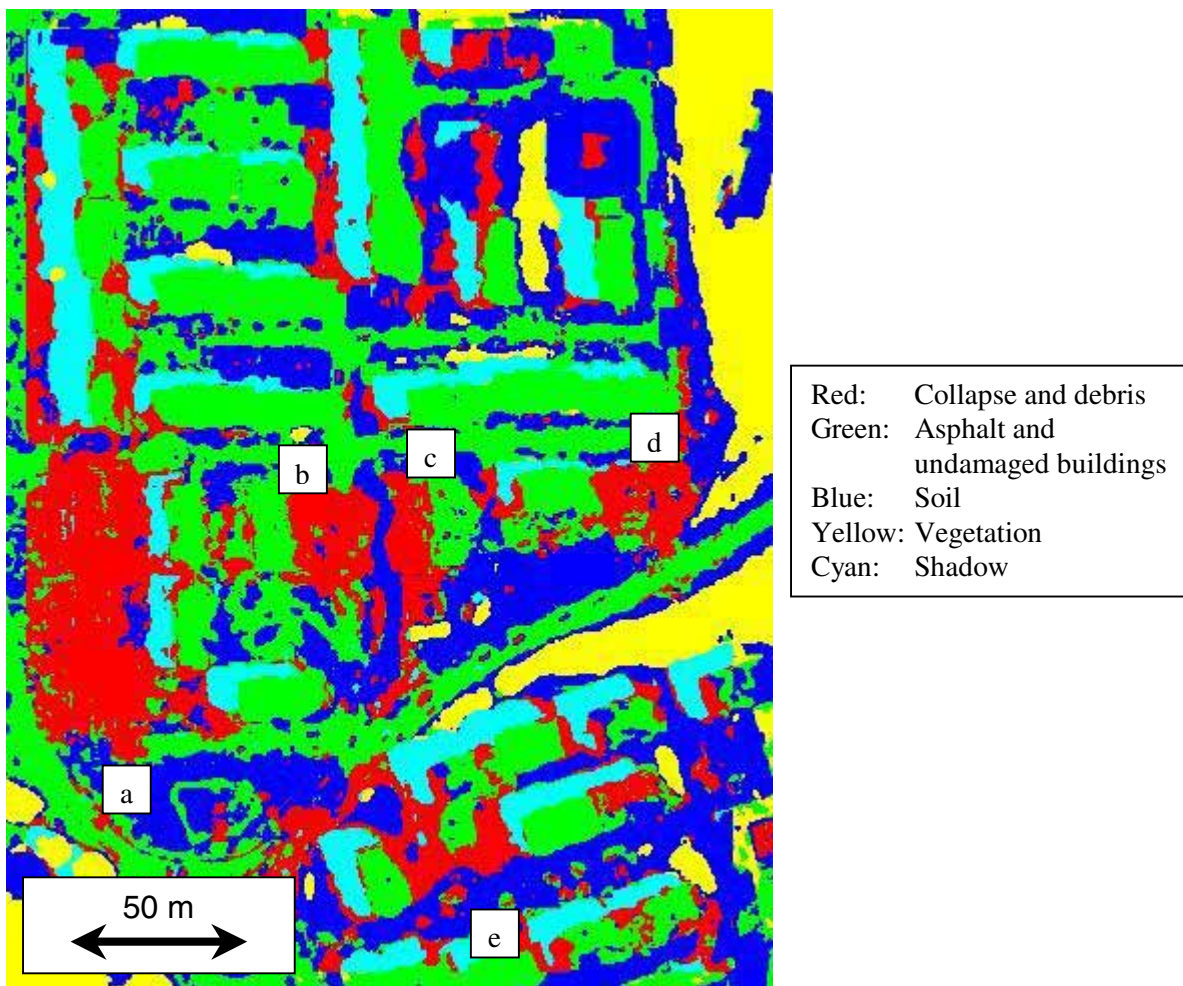


Figure 5. Classification results using CON and DIS textural measures and four spectral bands

image and do not confuse visual identification of the collapsed buildings. The final classification image allows the analyst to distinguish between zones with heavy damage (bottom of image) and zones with little damage (top of image). Most of the red areas in Figure 5 that do not correspond with collapsed buildings tend to represent areas with closely spaced cars that have textural and spectral characteristics that are similar to the collapsed areas.

Change Detection

As noted previously, change detection requires both pre- and post-earthquake satellite images. For the northern Algeria earthquake, one pre-earthquake image was available (22 April 2002), along with two post-earthquake images acquired about one month apart (23 May 2003, 18 June 2003). Typically, change detection requires co-registration of the images such that the same regions are compared in the two images. In this preliminary study, only visual change detection was considered (no co-registration required) in an effort to investigate: (1) the issues that may result in inaccurate damage identification from change detection, and (2) the information that potentially can be extracted using change detection that cannot be obtained from thematic classification.

Change detection algorithms identify all differences that are present between two images. When using change detection to distinguish regions damaged by an earthquake, it is important to consider what changes in the images are not due to the earthquake. This issue is particularly critical for high-resolution satellite images, which capture various features that are highly transient. For example, Figure 6 shows a region of Boumerdes acquired before (April 2002, Figure 6a) and after (May 2003, Figure 6b) the earthquake. Although these images represent the same section of the city, there are significant spectral and textural differences in the image. These differences are caused by a large collection of vehicles that were present in April 2002, but not in May 2003. Change detection methods would classify this part of Boumerdes as significantly changed, although the change was not caused by the earthquake. Other non-earthquake changes that may be identified by change detection algorithms include construction of new



Figure 6. Non-earthquake changes in satellite images acquired on (a) 22 April 2002 and (b) 23 May 2003.

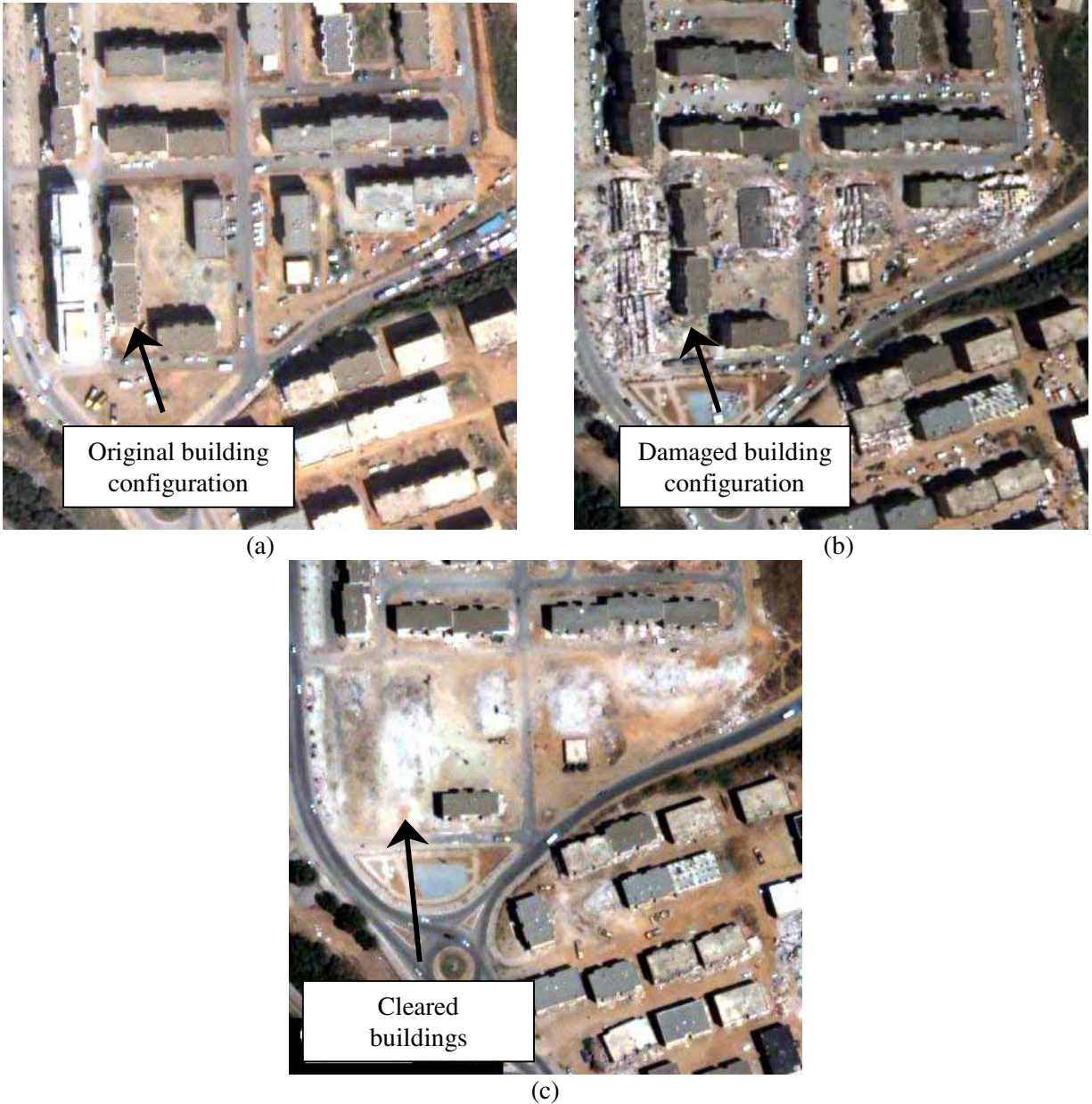


Figure 7. Identification of partially damaged buildings by comparing (a) 22 April 2002, (b) 23 May 2003, and (c) 18 June 2003 satellite images.

infrastructure, seasonal changes in vegetation, and partial cloud cover. Because of these issues, results from automated change detection results should be visually examined to ensure that the areas identified as changed were, in fact, changed by the earthquake.

Thematic classification of these images via the maximum likelihood method only allows fully-collapsed and pancaked buildings to be identified. Change detection can detect less dramatic damage because of the comparison between the pre-earthquake and post-earthquake configurations. Figure 7 again focuses on the damaged areas in southwestern Boumerdes. Figure 7a shows the pre-earthquake image, while Figures 7b and 7c are the post-earthquake images. If one considers only the 23 May 2003 post-earthquake image (Figure 7b), only the fully-collapsed buildings can be readily identified. No other damaged structures can be definitively identified. However, comparison of the 22 April 2002 image (Figure 7a) and the 23 May

2003 image (Figure 7b) reveals that the two buildings in the center of the image have translated significantly (approximately 5 m) from one another. This amount of movement is indicative of severe earthquake damage. This hypothesis is confirmed by the 18 June 2003 image (Figure 7c), which reveals that both of these buildings (along with the five fully-collapsed buildings) have been demolished and removed.

The 23 May 2003 and 18 April 2003 images represent an interesting opportunity to compare the damage information that is extracted immediately after an earthquake and about one month after an earthquake. The 23 May 2003 image, taken only two days after the earthquake, allows for a quick evaluation of damage shortly after the earthquake, which can be used in earthquake reconnaissance and recovery efforts. On the other hand, images taken weeks after an earthquake, while less useful in reconnaissance and recovery efforts, can identify buildings that have been demolished and removed after the earthquake (e.g., Figure 7c). It can be assumed that buildings that are removed after an earthquake experienced heavy earthquake damage. By documenting the buildings removed after an earthquake, a more complete picture of the damage patterns across a city can be developed.

For the small city of Boumerdes, it is possible to visual examine and compare the pre- and post-earthquake images to identify earthquake damage. Using the three satellite images acquired as part of this study, fully-collapsed and heavily-damaged structures were identified through visual examination. The resulting map of fully-collapsed (red) and heavily-damaged (yellow) structures is shown in Figure 8. This map clearly shows a concentration of damage in the southwestern part of the city. No heavily damaged buildings were identified in the northern or eastern sections of city, although moderate structural damage may have occurred in these areas. Unfortunately, earthquake reconnaissance reports published to date for the Northern Algeria earthquake [15] do not describe in the detail the damage patterns across Boumerdes, and therefore, the damage patterns in Figure 8 cannot currently be verified with ground truth data.



Figure 8. Collapsed (red) and heavily damaged (yellow) structures identified from visual examination of pre- and post-earthquake images.

If one assumes that the construction quality of structures across the city of Boumerdes is relatively uniform, owing to the fact that the city was constructed predominantly by government-owned contractors

[15], the concentration of damage in southwestern Boumerdes may be an indication of enhanced ground shaking due to soft soil conditions. A 1:500,000 scale geologic map of Algeria [Cornet 19] indicates that the majority of Boumerdes is founded on Pleistocene, lacustrine clays, with Quaternary alluvium found along river channels. The damaged areas in Figure 8 straddle the north-flowing river that runs through Boumerdes. Therefore, these areas may be underlain by younger alluvial sediments that amplified ground motions. Further investigation into the geology and soil conditions can confirm this hypothesis.

CONCLUSIONS

This study examined the potential use of high-resolution satellite images to identify earthquake-induced infrastructure damage. The city of Boumerdes, which was damaged during the 21 May 2003 Northern Algeria earthquake, was used as a testbed for this investigation. One pre-earthquake and two post-earthquake pan-sharpened images (0.6-m resolution) of Boumerdes were obtained and used to investigate earthquake damage detection using thematic classification of post-earthquake images and visual change detection using pre- and post-earthquake images.

Thematic classification of post-earthquake images involved identification of infrastructure damage (i.e., collapsed buildings) using spectral (color) and textural characteristics of damaged and undamaged areas. Initial classification using only spectral information did not clearly delineate the damaged and undamaged areas, because many undamaged areas had a spectral signature similar to that of the collapsed buildings. Including the texture measures contrast and dissimilarity to the classification process significantly improved the identification of collapsed structures.

Change detection algorithms that identify changed areas between pre- and post-earthquake images can provide a more-detailed representation of damage across a city. However, change detection using high-resolution images may be influenced by various changes not associated with the earthquake (e.g., vehicle congestion, clouds). This effect will result in areas erroneously identified as damaged by the earthquake. Visual examination of the pre- and post-earthquake images, including an image acquired almost a month after the earthquake, was used to develop a damage map of Boumerdes. This map reveals severe damage in the southwestern part of the city, which may indicate enhanced ground shaking in this area due to soft soil conditions.

The Northern Algeria earthquake represents the first earthquake captured by high-resolution satellite imagery. The results of this preliminary study indicate that these images contain a significant amount of information regarding the earthquake-induced damage to civil infrastructure. In future, these images will play a role in earthquake reconnaissance efforts, and will aid in identifying damage patterns across urban areas.

ACKNOWLEDGMENTS

The digital satellite images were obtained from Digital Globe and were purchased by the Earthquake Engineering Research Institute (EERI). Mr. Andy Dare of the University of Texas Center for Space Research performed the pan-sharpening of the images. Financial support was provided by the U.S. Geological Survey under NEHRP grant 04HQGR0072. This support is gratefully acknowledged.

REFERENCES

1. Schowengerdt, R.A. "Remote Sensing: Models and Methods for Image Processing." Academic Press, San Diego, CA, 1997.
2. Zhang, J. and Xie, L.- L. "Application of Recent Remote Sensing Technology in Earthquake Disaster Reduction." International Geoscience and Remote Sensing Symposium, IEEE, 2001: 3319-3321.
3. Haralick, R.M., Shanmugan, K., and Dinstein, I. "Texture Features for Image Classification." IEEE Transactions on Systems, Man, and Cybernetics, 1973, SMC-3: 610-621.
4. Julesz, B. "Experiments in the Visual Perception of Texture." Scientific American, 1975, 232: 34-43.
5. Weszka, J., Dyer, C., and Rosenfeld, A. "A Comparative Study of Texture Measures for Terrain Classification." IEEE Transactions on Systems, Man, and Cybernetics, 1976, SMC-6: 269-285.
6. Lamei, N., Hutchison, K., Crawford, M. M., and Khazenie, N. "Cloud Type Discrimination via Multi-Spectral Textural Analysis." Optical Engineering, 1995, 33: 1303 - 1313.
7. Fukuda, S. and Hiroswawa, H. "A wavelet-based texture feature set applied to classification of multi-frequency polarimetric SAR images," IEEE Transactions on Geoscience and Remote Sensing, 1999, 37(5): 2282-2286.
8. Derin, H. and Elliot, H. "Modeling of Segmentation of Noisy and Textured Images using a Gibbs Random Field." IEEE Trans. on Pattern Analysis and Machine Intelligence, 1987, PAMI-9: 39-55.
9. Manjunath, B.S. and Chellappa, R. "Unsupervised Texture Segmentation using Markov Random Fields." IEEE Trans. on Pattern Analysis and Machine Intelligence, 1991, PAMI-13:478-482.
10. Won, C.S. and Derin, H. "Unsupervised Segmentation of Noisy and Textured Images using Markov Random Fields." Comp. Vision, Graphics, and Image Processing, 1992, 54:308-328.
11. Bouman C. and Liu, B. "Multiple Resolution Segmentation of Textured Images" IEEE Transactions on Pattern Analysis and Machine Intelligence, 1991, 13: 99-113.
12. Krishnamachari, S. and R. Chellappa, R. "Multiresolution Gauss-Markov Random Field Models for Texture Segmentation," IEEE Transactions on Image Processing, 1997, 6:251-267.
13. Singh, A. "Review Article: Digital Change Detection Techniques Using Remotely Sensed Data." International Journal of Remote Sensing, 1989, 10(6): 989-1003.
14. Huyck, C.K., Mansouri, B., Eguchi, R.T., Houshmand, B., Castner, L.L., and M. Shinozuka, M. "Earthquake Damage Detection Algorithms using Optical and ERS-SAR Satellite Damage-Application to the August 17, 1999 Marmara, Turkey Earthquake." 7th National Conference on Earthquake Engineering, 2002, Boston, MA.
15. Earthquake Engineering Research Institute "The Boumerdes, Algeria, Earthquake of May 21, 2003," EERI Learning from Earthquakes Reconnaissance Report, EERI, 2003.
16. http://neic.usgs.gov/neis/eq_depot/2003/eq_030521/neic_ubbj_1.html
17. Research Systems, Inc. "ENVI. The Environment for Visualizing Images." Version3.4, Boulder, CO, 2000.
18. Lillesand, T., Kiefer, R., and Chipman, J. "Remote Sensing and Image Interpretation." 5th Edition, John Wiley & Sons, 2004.
19. Cornet, A. "Carte geologique de l'Algerie," Service de la carte geologique de l'Algerie, 1952.